A mossbauer study of ^{119}Sn in alloys of iron with Si, Al and Rh: interaction potentials and phase diagrams

1989 J. Phys.: Condens. Matter 1 829

(http://iopscience.iop.org/0953-8984/1/5/001)

J. Phys.: Condens. Matter 1 (1989) 829–846. Printed in the UK

A Mössbauer study of ^{119}Sn in alloys of iron with Si, Al and Rh: interaction potentials and phase diagrams

T E Cranshaw
Nuclear Physics Division, Harwell Laboratory, UKAEA, Oxon OX11 0RA, UK

Received 4 July 1988

Abstract. Mössbauer spectra of ^{119}Sn at a concentration of 0.2% in alloys of iron with Si, Al and Rh are presented. The strength of some of the interaction potentials between Sn and Si, Al and Rh are obtained, and some details of the iron-rich corner of the ternary phase diagrams elucidated.

In alloys of iron with silicon and aluminium, the interaction potentials are found to be large and positive, in agreement with the Miedema–Krolas and size-mismatch theories. We find that in both these alloy systems, the presence of tin in concentrations as low as 0.2% strongly lowers the value of the concentration of the alloying element at which ordered states of Fe_3Si and Fe_3Al appear.

In the iron–rhodium alloys, we find a potential at the first-neighbour distance between Sn and Rh atoms of −32 meV, in fair agreement with the Miedema–Krolas prediction of −84 meV. At the second-neighbour distance the potential cannot be determined. For Rh concentrations greater than 3%, an intermetallic compound is formed in which ^{119}Sn has a positive hyperfine field of 57 kOe and an isomer shift 0.1 mm s^{-1} less than is found at ^{119}Sn in iron.

1. Introduction

In previous papers (Cranshaw 1987a, b, hereafter called I and II), we have presented results on the interaction in solution in iron between ^{119}Sn atoms and atoms of most other elements which are soluble in iron. In this paper, we consider three solute elements, Si, Al and Rh, which were not included in I and II and have special points of interest.

Spectra of ^{119}Sn in iron alloys generally show broadened lines as compared with ^{119}Sn in pure iron, and occasionally recognisable or well resolved structure. We make the usual assumption that these effects are due to the presence of ^{119}Sn atoms with different near-neighbour environments, and in I and II found that invariably the presence of an atom of the alloying element in the first-neighbour shell of the ^{119}Sn atom reduced the absolute magnitude of the hyperfine field, whereas its presence in the second-neighbour shell caused an increase. Atoms in more distant shells (and sometimes in the first or second shell) cause changes which are sufficiently small compared with the linewidth to cause only a broadening of the lines.

Two models mainly distinguished by the range of the disturbance produced by the alloying element and described in detail in II were used to interpret the spectra. In model I, the value of ΔH_1, the change of hyperfine field produced by an alloying atom in the first-neighbour shell is large, so that a resolved component with a field ~10–20 kOe can

0953-8984/89/050829 + 18 $02.50

be seen. If a high-field component can be seen (>85 kOe) it is attributed to alloying element atoms in the second-neighbour shell. Atoms in the third-neighbour shell cause broadening of some of the lines. In model II, ΔH_1 is small, causing a broadening and perhaps some asymmetry of the lines, but further broadening by atoms in the third shell cannot be distinguished. These two models, modified when necessary by the inclusion of a further component to account for a second phase, form the basis of the interpretation of the spectra presented here.

The intensities of the components due to the presence of alloying atoms in the environment of the ^{119}Sn atom do not, in general, agree with the expectation derived from a random distribution, and in I and II we account for the departure by the interaction potential E_{b_i}, existing at the ith shell. Then the concentration C_i of alloying atoms in the ith shell is given by

$$\frac{C_i}{1-C_i} = \frac{C_\infty}{1-C_\infty} \exp(-E_{b_i}/kT) \tag{1.1}$$

where C_∞ is the concentration far from Sn atoms, k is Boltzmann's constant, and T is the temperature corresponding to the state of thermodynamic equilibrium existing in the specimen (I, II, Hrynkiewicz and Krolas 1983). If a specimen is allowed to cool from a high temperature, ($\gtrsim$900 K) diffusion will stop at about 700 K, so that the observed distribution of atoms is the frozen-in state corresponding to 700 K. If the specimen is rapidly quenched from a high temperature ($\gtrsim$1300 K), the temperature corresponding to the frozen-in state will be somewhat higher. Evidence has been presented in paper II that the effective quenching temperature may be about 900 K.

The origin of the interaction potentials is obviously an extremely complex question, but some progress can be made on the following simple lines. Krolas (1981, I) showed that at the first-neighbour distance, these potentials can be related to the heats of solution of the elements, if the heat of solution can be regarded as the result of a near-neighbour interaction. Miedema *et al* (1977) have given a semi-empirical theory which predicts the heats of solution of metals. We can use the two theories together to predict values of E_{b_1} which we call the Miedema–Krolas value, to compare with the measured values.

In I we studied s–p elements of the fourth period. We found that the interaction at first-neighbour distance was close to the Miedema–Krolas value, and the departures correlated with ΔV, the difference in atomic volume of the solute and host, iron. This may be interpreted as a consequence of size mismatch (Alonso *et al* 1985) and empirically the strength of the interaction is given by

$$E_{b_1}^{\text{size}} = -15.6\,(V_A - V_B)\ \text{meV} \tag{1.2}$$

where V_A, V_B are the atomic volumes of iron and tin respectively. At the second-neighbour distance, no correlation with the Miedema–Krolas value was found, as would be expected, but a good correlation was found with ΔV, suggesting that the interaction is largely due to size mismatch. In II, transition metals were studied with similar, but less persuasive results. The strength of the second neighbour interaction is given by

$$E_{b_1}^{\text{size}} = -36\,(V_A - V_B)\ \text{meV}. \tag{1.3}$$

In this paper, we present results on alloys of iron with Si, Al and Rh. These alloys behave rather differently from those described previously in that even at low concentration of the order of 5%, there is evidence of the appearance of a second phase. We are able to measure some of the interaction potentials, which we compare with the semi-empirical predictions described above.

It has been pointed out (Bläsius and Gonser 1976) that under favourable conditions when the Mössbauer isotope is present in low concentration, and shows different, easily recognised spectra in two phases, Mössbauer spectroscopy can be a very effective method of phase analysis. We show that these conditions are met in the alloys considered here, and are able to present some new details of the iron-rich corner of the ternary phase diagrams.

2. Experiment

The specimens were made by melting together the constituents in an argon arc furnace, and rolling down the resulting bead to 125 μm. Powder specimens were made by grinding with an emery wheel.

The spectra were taken in a conventional constant acceleration spectrometer at 77 K.

3. Silicon alloys

3.1. Results

Figure 1 shows spectra of ^{119}Sn in alloys of iron with 3, 4.5, 6, 7.5 and 9.0% silicon. In all cases, the tin concentration was nominally 0.2%.

The left-hand set of spectra are of specimens in the as-rolled state, and the right-hand set after the specimens had been annealed at 773 K for 410 h. The spectra of the as-rolled specimens show broadened lines and a high-field component visible as a shoulder on the spectra for $c = 3.0$, 4.5 and 6.0%, and as broadening for $c = 7.5$ and 9.0% Si. In the annealed spectra, the lines are somewhat narrower, the high-field component has disappeared, and a low- or zero-field component has appeared in the middle of the spectra. This component, with an isomer shift the same as that of the main component within the experimental accuracy, we attribute to the appearance of a second phase.

To interpret these spectra, we have little hesitation in attributing the high-field component to Sn atoms with Si atoms in the second-neighbour shell. If we were to choose model II, the broadening of the spectra mentioned above will be attributed to Si atoms in the first-neighbour shell, with small ΔH_1. Model I attributes the broadening to Si atoms in the third-neighbour shell, and we must then assume a strong repulsive interaction at first-neighbour distance which ensures that no first-neighbour pairs are observed. We find that the interpretation with model I gives more consistent values for the parameters than model II, and furthermore, is more consistent with the results for Al, given in § 4. Accordingly, we present the results of the analysis assuming model I.

Table 1 shows the values of the variables found by the fitting program for the as-rolled specimens, where we have assumed that the concentration of Si in the third-neighbour shell is the specimen concentration. Fitting the spectra for the annealed specimens then gives very similar results. If ΔH_3 is left fixed at 21.4 kOe, the mean of the values found in table 1 for the as-rolled specimens, and the concentration c_3 in the third-neighbour shell treated as a variable, c_3 for the annealed specimens comes out slightly below the specimen concentration. This gives the narrowing of the spectra noted above, and is consistent with the preferential removal of some Si into the second phase, leaving a lower silicon concentration in the solution phase.

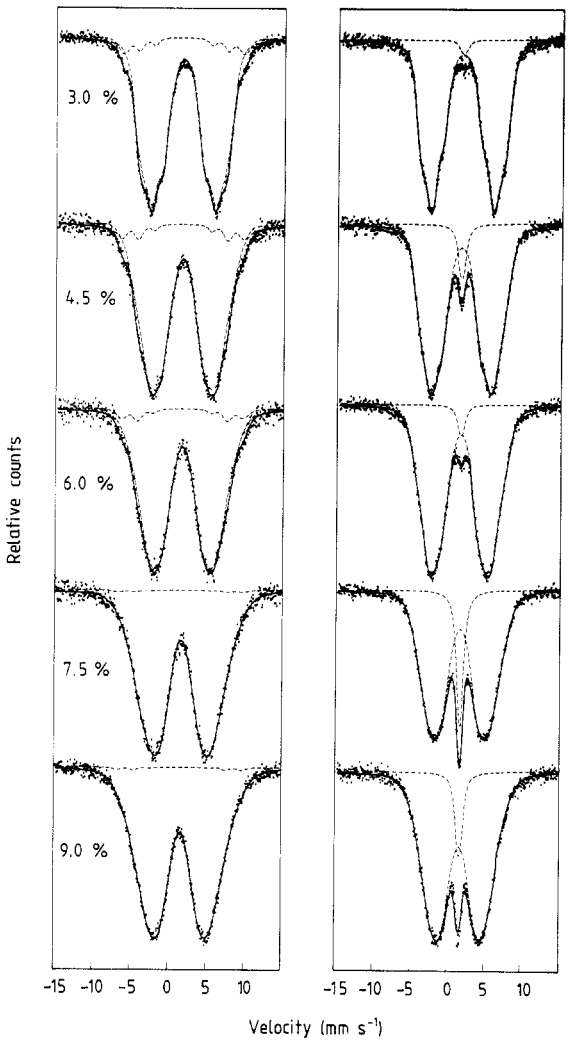

Figure 1. Spectra of ^{119}Sn in alloys of iron containing silicon at concentrations between 3% and 9%. The spectra on the left are of specimens in the as-rolled state, and on the right after annealing at 773 K for 410 h.

Table 1. The values of hyperfine parameters found by fitting the spectra of the as-rolled specimens in figure 1. H_{000} means the value of the hyperfine field for ^{119}Sn nucleus with no Si atom in the first three neighbour shells. All values are in kOe.

Concentration of Si(%)	H_{000}	ΔH_3	ΔH_2
3.0	−82	24	−34
4.5	−84	26	−32
6.0	−87	26	−30
7.5	−84	18	−36
9.0	−80	13	−40

Table 2. The relative intensity of the low-field component found in the annealed specimens of figure 1. All values are in per cent.

	Heat treatment			
Concentration of Si (%)	773 K 170 h	+773 K 240 h	+823 K 100 h	+873 K 100 h
3.0	5.6	1.9	1.2	0
4.5	8.2	6.0	1.0	0
6.0	8.3	3.3	1.0	0
7.5	12.6	13.4	6.6	2.4
9.0	6.5	7.9	10.9	8.7

Table 2 gives the relative intensity of the low-field component, attributed to a second phase, for the specimens after further heat treatments. It will be noticed that the intensity appears to behave in a rather inconsistent manner. For example, for the first three samples, the intensity falls after an additional 240 h heating at nominally the same temperature, whereas the fourth and fifth show an increase. Moreover, looking down the columns we notice that after 170 h and 410 h at 500 C, the intensity of the low-field component generally increases with silicon concentration, but the figures for the 6% and 9% specimens seem too low.

We believe these effects are due to the high sensitivity of the intensity of the low-field component to temperature and tin concentration, and to an increase in the time required to reach equilibrium as the silicon concentration is increased.

Although the nominal concentration of tin was the same, 0.2%, for all specimens, the tin was initially regarded as a probe, and not expected to have a serious effect on the behaviour of the alloy. Consequently, no special care was taken to keep the concentration the same in all specimens. For alloys of iron, silicon, and tin, x-ray fluorescence and the depth of the ^{119}Sn absorption in the Mössbauer spectra are good ways of estimating relative concentrations of tin. Using these methods, and assuming a mean concentration of 0.2% over all the specimens, we found for the 6% alloy a concentration of Sn of 0.15%, explaining the low weights of the low-field component for this alloy. The increase in the intensity of the low-field component in column 3 compared with column 2 for the 9% specimen may be due to small differences in temperature in different parts of the furnace, or to an increase in the time to reach equilibrium at high silicon concentrations.

3.2. Discussion

3.2.1. The ternary system Fe–Si–Sn. Figure 2 shows a part of the phase diagram of the FeSi system for Si concentrations less than 25% (Inden 1982). On it we have marked the results for the five alloys with 0.2% Sn used in this work, at temperatures of 773 and 873 K. We have drawn open circles for the two phase alloys and full circles for the solution state, and between them we have drawn a plausible boundary line. It would appear from figure 2 that the addition of 0.2% Sn has moved the two-phase boundary very substantially towards lower silicon concentrations.

Evidence has been presented in the past of a strong repulsive interaction between silicon atoms at first- and second-neighbour distances, leading to the hypothesis of the

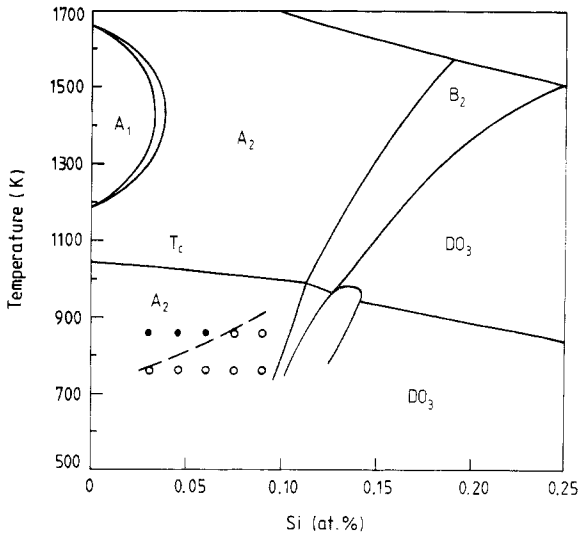

Figure 2. Part of the phase diagram of iron–silicon alloys. The results of the present investigation are shown as full circles for single-phase alloys, and open circles for two-phase alloys.

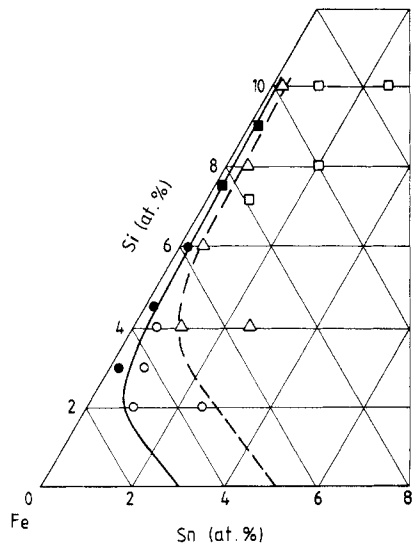

Figure 3. The ternary phase diagram for Fe–Si–Sn at 873K. The open symbols are from Vogel and Jungclaus, triangles for single-phase solution, squares and circles for two-phase. The full symbols represent the present results. Circles indicate single-phase solution, squares two-phase state.

existence of a $Fe_{15}Si$ ground state for dilute silicon alloys (Cranshaw *et al* 1966, Cranshaw 1977, Japa and Krop 1978). The present results suggest an even stronger repulsion between silicon atoms and tin atoms.

The ternary system Fe–Si–Sn has been studied by Vogel and Jungclaus (1960). Their conclusions for concentrations of Si and Sn less than 10% are illustrated in figure 3, taken from their figure 14 by converting the scales in weight per cent to atomic per cent. They distinguish three states; solution, two phase and tin precipitation, marked in the figure by open triangles, squares and circles respectively. They call the figure a 'room temperature' diagram, but it must clearly correspond to some higher temperature at which a state near thermal equilibrium has been reached. They draw a boundary line between the

solution phase and the other two states reproduced as a broken curve in figure 3. On the tin axis, it passes through the point 5%, indicating a solubility for tin in iron of 5%.

At the date at which their work was done, the accepted value of the solubility of tin in iron was about 5% at 673 K (Hansen and Anderko 1958), but more recent work indicates a much lower figure (Nageswararao *et al* 1974), and the solubility at 873 K is found to be 3.2%. Accordingly, we have marked on figure 3 the three solution phase and two two-phase points found in the present work for silicon alloys with 0.2% tin at 873 K and drawn a boundary passing between these points and through 3.2% on the tin axis. This we believe indicates the boundary for 873 K.

It is difficult to be precise about the nature of the second phase observed in these spectra. The amount of transformed material is of the order of one part in 10^4, so that we would not expect it to be seen in a ^{57}Fe spectrum of the same material. Vogel and Jungclaus claimed to see precipitated tin in their specimens; we certainly do not see a tin phase in this work, but this could be due to the low f factor for metallic tin compared with tin in solution in iron.

It is relevant here to refer to the work of Delyagin and Kornienko (1972). These authors prepared specimens of a solution of ^{119}Sn in ordered Fe_3Si, and observed ^{119}Sn with a hyperfine field of -50 kOe. They remark that the solubility of tin in Fe_3Si is less than 0.2%. At greater concentrations they found in their spectrum a line corresponding to a non-magnetic phase, which might be the same as the second phase found here. We can reconcile these observations in the following way.

It is well known that the BCC lattice can be regarded as the superposition of four FCC sublattices. In Fe_3Si, one of these sublattices is called Fe I, on which Fe atoms are second neighbours to Si atoms, two crystallographically equivalent sublattices are called Fe II on which Fe atoms are first neighbours to Si atoms, and the fourth is occupied by Si atoms. Tin atoms could lie on any of these sublattices.

At low concentrations of silicon, as in our case, it is natural to suppose that Sn atoms in the DO_3 phase would occupy Si sites, because then they would not be nearer than third neighbour to Si atoms. They may there have a hyperfine field near zero. At Si concentrations at 25%, as in the work of Delyagin and Kornienko, it may be that the Sn atoms are forced to occupy Fe I sites, where they would be second neighbours to Si atoms and there they may have a hyperfine field of -50 kOe. At tin concentrations greater than 0.2%, there may be a distribution of tin atoms on Si sites and Fe I. Such effects would reconcile our observations with those of Delyagin and Kornienko.

3.2.2. Hyperfine parameters. The hyperfine parameters given in table 1 show a good deal of scatter, as might be expected from the rather broad lines shown in figure 1. For the as-rolled specimens both models I and II suggest that the field at ^{119}Sn atoms which have no Si atom in the first three shells, shows no clear trend with concentration, but may decrease slowly from -82 kOe to about -80 kOe with addition of Si, and the same dependency may be observed in the annealed specimens. The value of ΔH_2, the change brought about by the presence of a Si atom in the second-neighbour shell, may show a small increase, from about -34 kOe to -40 kOe, but a constant value would fit the data almost as well.

These results are in marked contrast with those of Dubiel and Zinn (1982), who have interpreted alloy spectra similar to the ones presented here by assuming that there is a random distribution of Si atoms in the first- and second-neighbour shells of the Sn atom, and that ΔH_1 and ΔH_2 are both positive. They find that the absolute magnitude of the field at Sn atoms which have no Si atom in the first- or second-neighbour shell increases

from 83 kOe to 105 kOe at a Si concentration of 9%. We believe this apparent increase is due to the occurrence of Sn atoms with Si atoms in the second-neighbour shell, for which ΔH is negative.

3.2.3. Interaction potentials. We have given reasons for believing that even in the as-rolled specimens, the repulsion between tin and silicon atoms at the first-neighbour distance is large enough to make the number of Si–Sn first-neighbour pairs unobservable. By comparison with alloys of iron and gallium or germanium, a repulsive potential substantially greater than 200 meV is indicated. The predicted Miedema–Krolas value is indeed 196 meV, and the size mismatch component predicted by equation (1.2) is 78 meV.

At the second-neighbour distance, according to the results of papers I and II only the size mismatch component exists, and the predicted value of equation (1.3), is 180 meV. Again, this is consistent with the measurements, because although the presence of Si–Sn pairs at the second-neighbour distance was easily seen in the rolled specimens, it was undetectable in the annealed specimens.

3.3. Conclusions

We have presented spectra of ^{119}Sn in solution in iron–silicon alloys with silicon concentration between 3% and 9%. The following conclusions are deduced from an analysis of the spectra.

(i) There exist interaction potentials between Si and Sn atoms dissolved in iron of magnitude >200 meV at first-neighbour distance, and about 180 meV at the second-neighbour distance. These results are in good agreement with the empirical predictive methods developed in I.

(ii) The change of field at ^{119}Sn nuclei produced by a Si atom in its first-neighbour shell could not be determined because there are too few such pairs in the specimen. The change produced by a Si atom in the second-neighbour shell, ΔH_2, is −34 kOe.

(iii) In the ternary phase diagram, the region of single-phase solution is strongly reduced by the addition of tin. At 873 K, 0.2% Sn lowers the single-phase boundary from a silicon concentration of 11% to 7%, and at 773 K, from 10% to less than 3%.

4. Aluminium alloys

4.1. Results

Figure 4 shows the spectra of ^{119}Sn in an alloy of iron with 3% Al after the foil had been given a range of different heat treatments. The spectrum marked ASR is the spectrum of the specimen in the as-rolled state, and the next three spectra were obtained after annealing for 3 h at 473, 573 and 673 K, respectively. The remaining two spectra were obtained after annealing at 723 K for three and fifteen days. Figure 5 shows spectra of a powder sample of the same alloy, in the as-ground state, and after annealing at 723 K for 16 h.

The area of doubt in the interpretation of the spectra of the aluminium alloys is somewhat less than in the case of the silicon alloys because in the aluminium alloys, the presence of a component attributable to Sn atoms with a first-neighbour Al atom can be observed with some confidence in the as-rolled specimens, and specimens annealed at

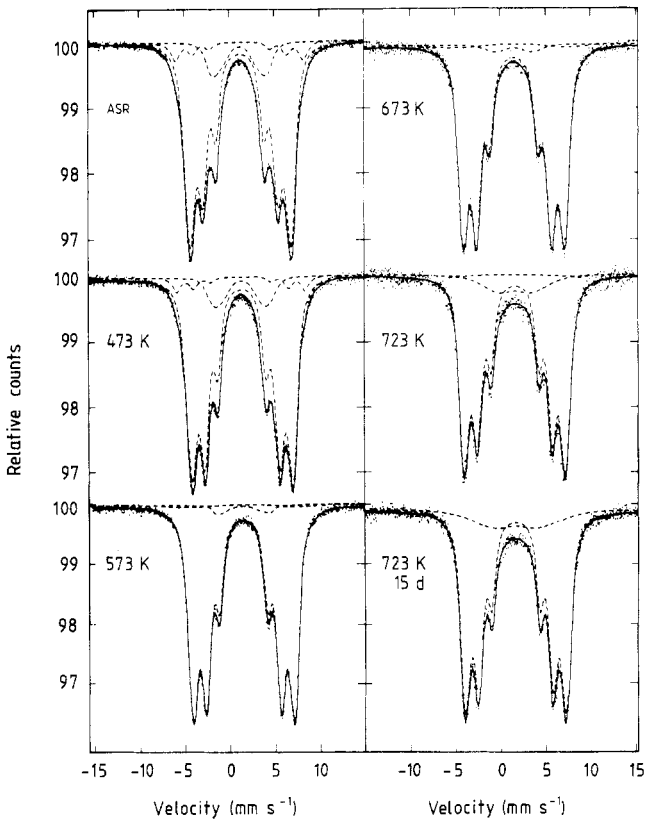

Figure 4. Spectra of ^{119}Sn in alloy of iron with 3% Al, in the as-rolled state and after annealing for different periods at a range of temperatures.

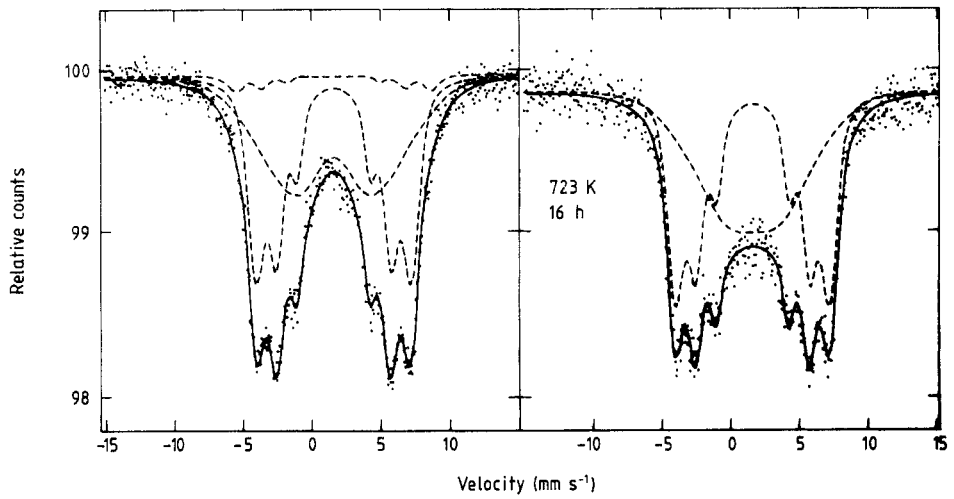

Figure 5. Spectra of ^{119}Sn in alloys of iron with 3% Al in the as ground state and after annealing for 16 h at 723 K.

temperatures less than 573 K. We therefore use model I of paper II, as in the silicon case, but permitting the existence of a first-neighbour component.

Table 3 gives the results of the fitting. For the first shell, we give the strength of the field, the intensity of the component in the spectrum, and a parameter σ which is the best value of a Gaussian component folded with the natural Lorenz width. For the second shell, we give the value of the field and the component intensity, and for the third shell, we assume that the concentration in the shell is the sample concentration, as for the silicon case. The value of ΔH_3 can then be found by the fitting program, and we give this value. Because these two quantities cannot be determined independently, they are given in brackets in table 3.

Table 3. The values of parameters found by fitting the spectra of figures 4 and 5. Reasons are given in the text for renaming the low-field component '2nd phase'.

Heat treatment		1st shell			2nd shell		3rd shell	
		H (kOe)	Intensity (%)	σ (kOe)	H (kOe)	Intensity (%)	ΔH_3 (kOe)	Concentration of Al (%)
Foil								
ASR		−46	11	4.3	−104	6.6	(6)	(3.0)
2 h	473 K	−46	10	4.9	−103	4.0	(5)	(3.0)
2 h	573 K	−43	2.4	5.4	−102	1.2	(7)	(3.0)
2 h	673 K	−39	2.2	14	−103	1.5	(6)	(3.0)
2nd phase								
3 d	723 K	−31	10	26	—	(0)	(6)	(3.0)
15 d	723 K	−45	12	36	—	(0)	(5)	(3.0)
2nd phase								
Powder								
As ground		−25	46	35	104	3.4		
16 h	723 K	−40	47	39	—	(0)		

Looking down the columns, we find that the intensity of the component attributed to first-neighbour Al atoms drops sharply after the anneal at 573 K, remains the same for the 673 K anneal, and then rises after a 723 K anneal. We attribute the fall in the intensity to a strong repulsion between Sn atoms and Al atoms at the first-neighbour distance, which reduces the number of Sn–Al pairs during the anneal, and the subsequent increase to the production of a second phase in the specimen after annealing at 723 K. We have accordingly changed the label in the table to 'second phase'. This interpretation receives some confirmation from the fact that σ, which measures the excess width of the lines over the Lorenz width rises rapidly from about 5 kOe, a value barely experimentally distinguishable from zero, to values between 14 and 39 kOe. The change is visible to the eye in the spectra of figure 4, and is particularly clear in the spectra of the powder sample in figure 5. To investigate this interpretation further, we took spectra of ^{57}Fe in the powder sample,

Figure 6 shows the ^{57}Fe spectrum of the powder sample after annealing at 723 K for 16 h. The spectrum has been fitted as a superposition of three magnetically split spectra.

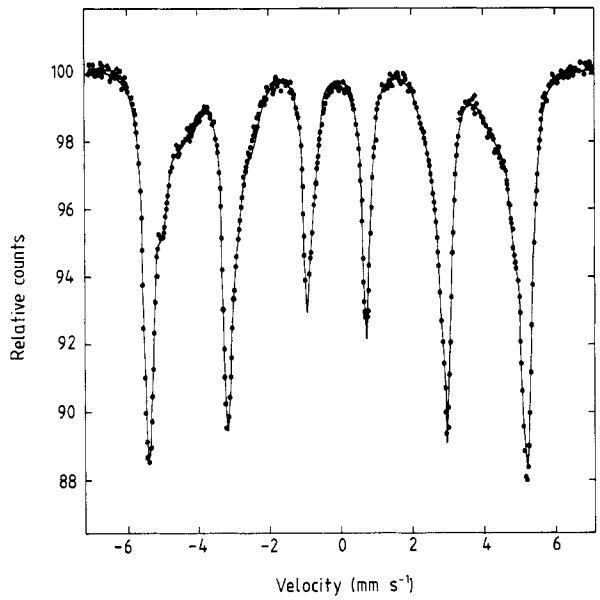

Figure 6. Spectrum of ^{57}Fe in the annealed powder sample, showing the existence of two phases.

Two components have narrow lines, with fields of −330 kOe and −305 kOe, and isomer shifts of 0.0 and 0.016 mm s^{-1}. These lines with relative intensities 88 : 12 can be attributed to isolated iron atoms and iron atoms with an Al atom in the first-neighbour shell respectively. The ratio of intensities corresponds to an Al concentration of 1.6%. The third component is satisfactorily represented by a normal distribution of fields with a mean of 282 kOe and a standard deviation of 23 kOe. The total spectrum can therefore be interpreted as that of a two-phase state, one of which is a simple solution of Al in Fe, and the other a more complex component probably with Fe_3Al order. The ratio of the numbers of iron atoms in the two phases is 75.5 : 24.5. From these figures we calculate that the concentration of Al in the second component is 8.2%.

An x-ray diffraction picture of the powder showed the patterns of two BCC lattices, one, the stronger of the two, with a lattice parameter of 2.870, and the weaker with a lattice parameter of 2.901. The latter value is rather high for Fe_3Al, and certainly unexpectedly high for a component with DO_3 order but only 8.2% Al and 0.2% Sn. Nevertheless, this does seem the most likely interpretation of the spectrum.

4.2. Discussion

4.2.1. The ternary system Fe–Al–Sn. As in the case of silicon alloys, we can interpret these results as a consequence of the shifting of the boundary between the solution phase and the two-phase state to lower solute concentrations by the addition of 0.2% Sn. Figure 7 shows a part of the iron–aluminium phase diagram, for Al concentrations less than 25% (Kubaschewski 1982). If we assume that the powder specimen annealed at 723 K is in equilibrium, we have determined for the alloy containing 0.2% Sn two points on the two-phase boundaries, at 1.6% and 8.2%. We have marked these points on figure 7 and drawn plausible boundary lines through them.

We may note a difference between the Al and Si results. In the case of the Si alloys, we believed that only a small part of the material was in the DO_3 form, because the ^{57}Fe

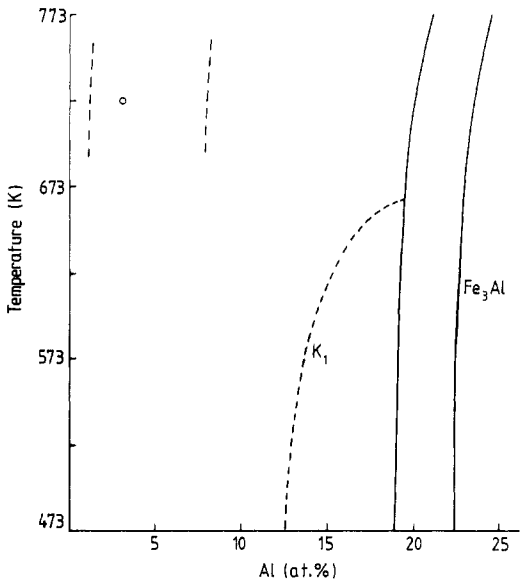

Figure 7. A part of the phase diagram of FeAl alloys.

spectrum showed only the usual spectrum for a solution of silicon in iron. This implies that the boundary between the two-phase state and the DO_3 phase is close to Fe_3Si. For the Al alloys, on the contrary, a large part of the material is in the DO_3 phase, and the boundary between the DO_3 phase and the two-phase state must be far from Fe_3Al, in fact at 8.2%. The component observed in the ^{57}Fe spectrum due to the DO_3 phase is unfortunately too broadened to permit confirmation of this point from a detailed fitting.

The striking difference between the spectra of the rolled specimens and the ground specimens is interesting. In all the iron alloys studied here or in papers I and II, the rolled specimen is in a state nearer random solution than the state reached by low-temperature annealing. When the temperature of a rolled specimen is raised so that diffusion occurs, the structure shifts to a more ordered state. This implies that the rolled state corresponds to a quenched-in state at a temperature higher than the temperature at which significant diffusion occurs in a time of the order of hours.

It is not obvious that this should always be so. In the deforming material at the point of rolling, relatively large amounts of energy are available, and high densities of dislocations and vacancies must be produced. It is certainly conceivable that, at least for short ranges to which the Mössbauer spectra are sensitive, the rolling process would make low-temperature ordered states accessible, just as does irradiation with fast particles, but this never seems to occur in iron alloys.

The case of grinding or powdering with an emery wheel as we have carried out in the present experiments may be more complicated. Not only is there heavy deformation and 'cold work', but particles may be produced at high temperatures and rapidly quenched. The Mössbauer spectra seem to indicate that the ground particles are in a more ordered state than the rolled specimens in the sense that there is present a larger proportion of the DO_3 state, but that a comparable degree of disorder is present as judged by the presence of Sn atoms with Al atoms at the second-neighbour distance. These pairs were broken up by annealing at 723 K, as can be seen in the last line of table 3.

4.2.2. Hyperfine parameters. The value of the hyperfine field in the first four rows of table 3 are comparable with the values found for the other elements in papers I and II and unremarkable, but the value found for the ^{119}Sn hyperfine field in the second phase needs some comment.

As for the silicon alloy, we may refer to the work of Delyagin and Kornienko (1972). These workers found a somewhat greater solubility for Sn in Fe_3Al than in Fe_3Si, but a great sensitivity of the ^{119}Sn spectrum to the stoichiometry and to mechanical working. The strength of the field at ^{119}Sn in Fe_3Al was found to be +8.5 kOe.

We unfortunately do not know the sign of the field found in our second phase, but in table 3 have assumed it to be negative. As in the case of the silicon alloys, we may then suppose that the field at ^{119}Sn on Al sites where the nearest-neighbour alloying atom is in the third neighbour shell is about −35 kOe, but on the Fe II site it may have the value +8.5 kOe.

4.2.3. Interaction parameters. We have noted in table 3 that in the as-rolled specimens, the intensity of the component attributed to first-neighbour Al atoms is about 10.5%, but after annealing at 573 K, it falls to 2.4%, a figure which is, in fact, too low to be determined accurately. These figures lead to values of c_1, the alloy concentration in the first-neighbour shell of a Sn atom of 1.32% and 0.3%. From the first figure, we can say only that the repulsion at the first-neighbour distance is less for Al atoms than for Si atoms. From the second, we deduce a value for E_{b_1} of 114 meV. The Miedema–Krolas theory predicts values of 196 meV for Si–Sn, and 150 meV for Al–Sn, and equation 1.2 gives values of 77 meV and 45 meV for the size-mismatch component. Our observations are therefore in agreement with the theory as to the direction of the change in going from Si to Al, and in fair agreement with the absolute value for Al–Sn.

At the second-neighbour distance, the information available here is scarcely sufficient to deduce a value for the interaction potential. The values for the intensity of the second-neighbour component in table 3 lead to a value of +135 meV. The predicted value from the size mismatch using equation (1.3) is +104 meV.

4.3. Conclusions

We have presented spectra of ^{119}Sn dissolved in alloys of iron–3% aluminium. The specimens were in the form of foil or powder, and were given a range of heat treatments.

(i) There exist interaction potentials between Al and Sn atoms dissolved in iron, of magnitude approximately 114 meV at the first-neighbour distance, and 135 meV at the second-neighbour distance. The predicted values by the methods of paper I are 150 meV and 104 meV.

(ii) The field at a Sn nucleus when the atom has a first-neighbour Al atom is −44 kOe, i.e. ΔH_1, the change produced is +39 kOe. The change produced by an Al atom in the second-neighbour shell is −20 kOe.

(iii) In the ternary phase diagram, the single-phase solution region is strongly reduced by the addition of 0.2% Sn. At 673 K, the solution phase boundary occurs at about 1.6% Al instead of 18% in pure iron–aluminium alloy.

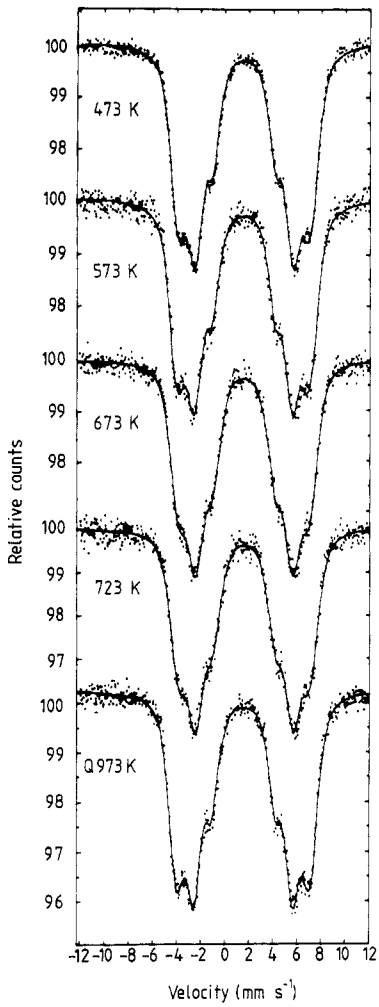

Figure 8. Spectra of ^{119}Sn in alloy of iron with 2% rhodium, after different heat treatments.

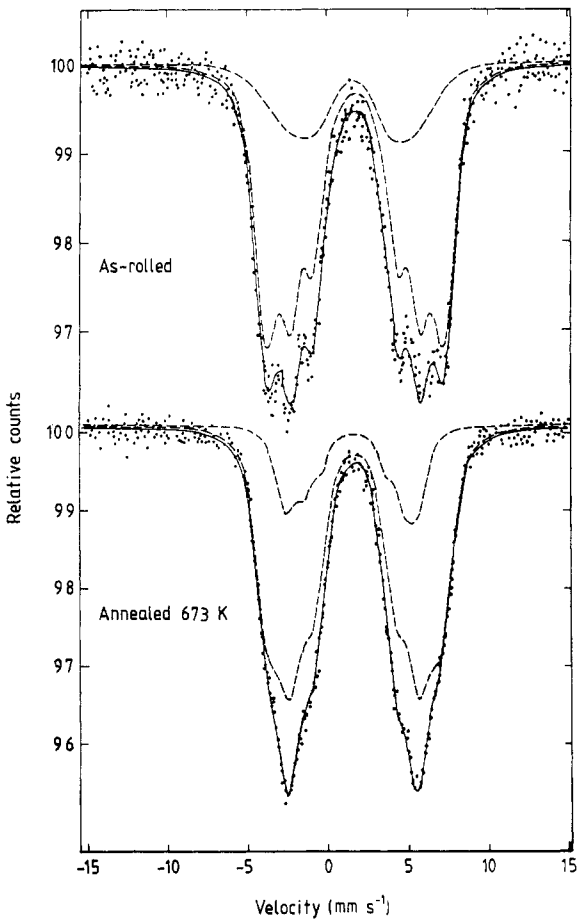

Figure 9. Spectra of ^{119}Sn in alloy of iron with 2% rhodium, after different heat treatments.

5. Rhodium alloy

5.1. Results

Figure 8 shows spectra of ^{119}Sn in an alloy of iron with 2% rhodium, after annealing for 3 h at 473 K, 573 K, 673 K and 725 K. The last spectrum was obtained after quenching the specimen from 973 K. The spectra resemble those of tin in pure iron, but with broader lines.

On examining the spectra in more detail, we may notice that a slight change towards an increasing absorption at low velocities occurs between 573 K and 673 K, resulting in broader lines. There is a return to narrower lines on quenching from 973 K. This behaviour is typical of elements for which an attractive potential exists for tin at the first neighbour distance, resulting in an increase in the number of

neighbour atoms on annealing. Accordingly, we fit the spectra using model II of paper II.

The data are insufficiently accurate to permit the simultaneous determination of c_1, the Rh concentration in the first-neighbour shell, and ΔH_1, the change of field produced at the ^{119}Sn nucleus by the presence of a Rh atom in its first-neighbour shell. Consequently, we assume that in the as-rolled specimen, the value of c_1 is 2.0%, the same as the sample concentration. This permits a determination of ΔH_1.

We can then use this value of ΔH_1 to find the concentration of Rh in the first shell of a Sn atom after heating at a high enough temperature for diffusion to occur. The values found are $c_1 = 3.6$ and 3.2%, leading to values of the attractive potential in the first shell of the Sn atom of −34.1 and −29.3 meV for the anneals at 673 K and 723 K respectively. The average of these values is −31.7 meV, and we believe this to be a more accurate determination than the value −14 meV given in paper II, which was based on the spectrum of a quenched specimen only.

Figure 9 shows spectra of ^{119}Sn in iron–3% Rh, in the as-rolled state, and after annealing at 673 K for 2 h. The first spectrum is clearly asymmetric to the eye, and we deduce the existence of components which were not present in the spectra of figure 8. Further information about these components can be found by considering the spectra shown in figure 10, which again shows spectra in the as-rolled state and after heating at 673 K for 2 h, but now the Rh concentration is 6%. The spectrum of the as-rolled specimen shows a remnant component with a field of about 83 kOe, but a larger component with a smaller field. In the annealed specimen, the higher field component has disappeared. The spectra are distinctly asymmetric, even when the contribution from Sn in solution in FeRh alloy is small, as in the annealed specimen. We suppose the new component is due to the presence of an intermetallic compound, in which the Sn atoms are in a non-cubic environment leading to a quadrupole interaction as well as a magnetic hyperfine field. The application of an external field of 6 kOe shows that the strength of the magnetic hyperfine field in this compound is +57 kOe. The shift of the magnetic lines by the quadrupole interaction is −0.04 mm s^{-1}, and the isomer shift is −0.1 mm s^{-1} relative to the shift for Sn in iron.

In some spectra, the intermetallic compound gives some evidence of a second tin site with an intensity of 15% of the component described above, and a hyperfine field of 32 kOe, but confirmation could not be obtained in all cases.

5.2. Discussion

5.2.1. The Fe–Rh–Sn system. In the FeRh system, an ordered CsCl state is known to occur, but the boundary of the solid solution phase and two-phase state, which may be at about 10% Rh, is uncertain (Swartzendruber 1984). The RhSn system shows several intermetallic compounds, of which the richest in Rh is Rh_2Sn (Hansen and Anderko 1958).

With the meagre amount of information provided by the present results, we can only sketch a hypothetical ternary phase diagram for the temperature 673 K as shown in figure 11, in which the three alloys studied here are marked by dots. A broken curve divides the solution state from a two-phase state. Somewhere off the diagram is an undetermined ternary intermetallic compound. The compound Rh_2FeSn has been investigated by Suits (1976). It has a Heusler alloy type of structure with a strong tetragonal distortion, which would be consistent with the EFG observed in the present spectra.

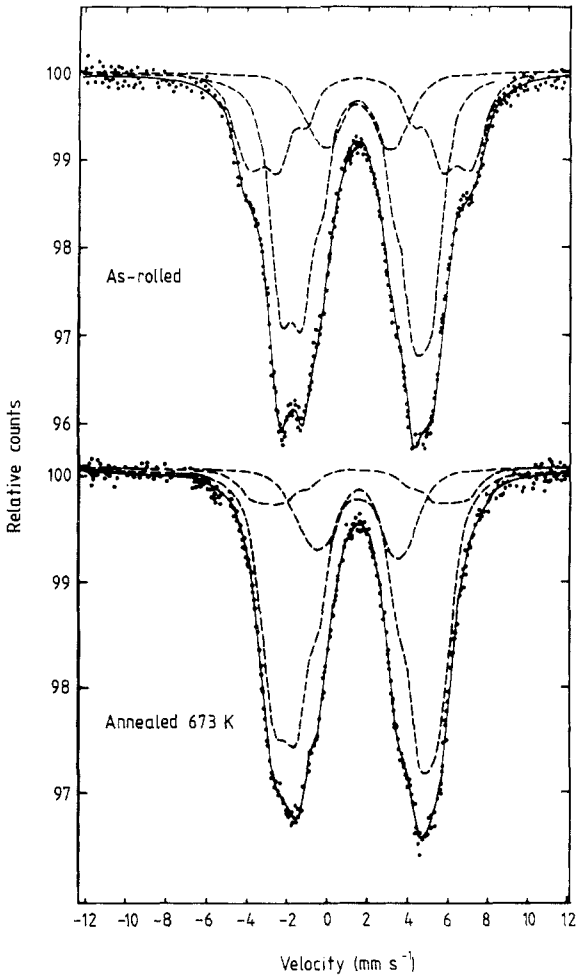

Figure 10. Spectra of ^{119}Sn in alloy of iron with 6% rhodium in the as-rolled state, and after annealing for 2 h at 673 K. The annealed spectrum shows almost no component corresponding to the solution phase.

5.2.2. Hyperfine parameters. In none of the spectra is there any component with a field greater than 82 kOe, which we have always interpreted as due to Sn atoms with an alloying element in the second-neighbour shell. The failure to observe such a component may indicate that there is a strong repulsive interaction at the second neighbour distance, or that ΔH_2, the change of hyperfine field produced by the presence of a Rh atom in the second shell is small. The latter would not be surprising, because the Rh atom itself carries a moment, and may increase the moment on neighbouring iron atoms. The value of ΔH_1 is rather poorly determined in the spectra, but is found to be about +20 kOe.

The existence of a positive hyperfine field at the ^{119}Sn nucleus in the intermetallic compound is interesting. We have observed positive values of the field for Sn in FePd alloys (Cranshaw 1980) when the Sn atom has more than about four Pd atoms in its first-neighbour shell. This suggests that in the intermetallic compound, Rh atoms may occupy near-neighbour positions, while Fe atoms are at greater distances. The change of isomer shift of -0.1 mm s^{-1} in the intermetallic compound is also noteworthy,

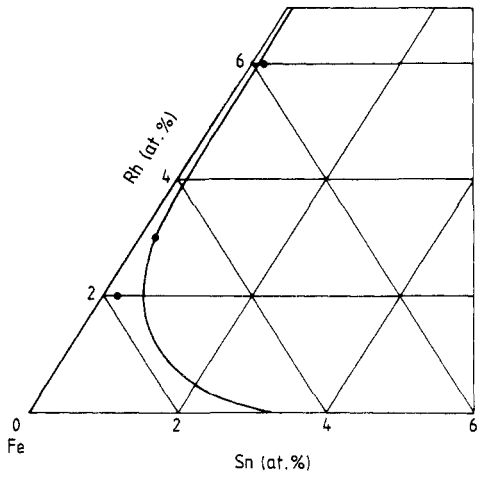

Figure 11. The ternary phase diagram of Fe–Rh–Sn for a temperature about 673 K.

because we have found no changes of isomer shift in other dilute iron alloys, and may also be associated with Rh atoms as near neighbours.

5.2.3. Interaction potentials. We have described in § 5.1 the deduction of the value −32 meV for the first-neighbour interaction potential. It will be noted that this value assumed that the as-rolled specimen was a random solution. The failure of this assumption would mean that the interaction potential was more negative than −32, but the error is not likely to be great. The Miedema–Krolas prediction is −84 meV, and the size mismatch component given by equation (1.2) is +18 meV, in fair agreement with the experimental value.

The second-neighbour potential cannot be determined for the reasons given in § 5.2.2.

5.3. Conclusions

We have presented spectra of ^{119}Sn atoms in solution in alloys of Fe with 2%, 3% and 6% Rh, and reached the following conclusions.

(i) The interaction potential between Sn and Rh atoms at the first-neighbour distance is −32 meV. We are unable to deduce any value for the interaction at second-neighbour distance.

(ii) The change in hyperfine field at ^{119}Sn due to the presence of a Rh atom as first neighbour is $\Delta H_1 = +20$ kOe. We are unable to deduce any value for ΔH_2.

(iii) For concentrations of Rh > 3% and of Sn of 0.2% at 400 °C an intermetallic compound is formed in which the hyperfine field at the ^{119}Sn nucleus is +57 kOe and the isomer shift is −0.1 mm s^{-1} relative to tin in iron.

Acknowledgments

It is a pleasure to thank M Rand for many helpful discussions, L Bint for the preparation of the FeBeSn sample, and L Becker for taking the spectra. The work described in this paper is part of the longer term research carried out within the underlying programme of the UKAEA.

References

Alonso J A, Cranshaw T E and March N H 1985 *J. Phys. Chem. Solids* **46** 1147
Bläsius and Gonser 1976 unpublished
Cranshaw T E 1977 *Physica* B **86–88** 391
—— 1980 *J. Phys. F: Met. Phys.* **10** 1323
—— 1987a *J. Phys. F: Met. Phys.* **17** 1645
—— 1987b *J. Phys. F: Met. Phys.* **17** 2475
Cranshaw T E, Johnson C E, Ridout M S and Murray G A 1966 *Phys. Lett.* **21** 481
Delyagin N N and Kornienko E N 1972 *Sov. Phys.–JETP* **34** 1036
Dubiel S M and Zinn W 1982 *J. Magn. Magn. Mater.* **28** 261
Hansen M and Anderko K 1958 *Constitution of Binary Alloys* (New York: McGraw-Hill)
Hrynkiewicz A Z and Krolas K 1983 *Phys. Rev.* B **28** 1864
Inden G 1982 *Bull. Alloy Phase Diagrams* **2** 419
Japa E and Krop K 1978 *Phys. Status Solidi* a **50** K89
Krolas K 1981 *Phys. Lett.* **85A** 107
Kubaschewski O 1982 *Iron Binary Phase Diagrams* (Berlin: Springer) p 6
Miedema A R, de Boer F R and Boom R 1977 *Calphad* **1** 341
Nageswararao M, McMahon C J and Herman H 1974 *Metall. Trans.* **5** 1061
Suits J C 1976 *Solid State Commun.* **18** 423
Swartzendruber L J 1984 *Bull. Alloy Phase Diagrams* **5** 456
Vogel R and Jungclaus H J 1960 *Arch. Eisenhüttenwesen* **31** 243